I J C T A, 9(6), 2016, pp. 2911-2922 ISSN: 0974-5572

MPPT Based Autonomous PV Module with Sensor Less Control of BLDC Motor for Maximum Solar Power Generations

Sundaram A.* and G.P. Ramesh**

ABSTRACT

This Paper presents the efficient power generation of Photovoltaic System and also deals with the sensor less control of BLDC motor. The controller design of an Autonomous PV Module (APVM) has found a lot of attentions in maximum power point tracking (MPPT) for PV system applications. It consists of a PV panel and a Non-inverting Four Switch buck-boost Converter (NFSBBC) for maximum power generations. The mathematical model of single diode Photovoltaic cell has found to be better and accurate at wide variations of irradiance and temperature. This NFSBBC can be operating in buck, boost and buck–boost modes addition with reduced number of passive devices and non-inverted output voltage polarity. The sensor less control of BLDC motor based on a hysteresis comparator and a potential start-up method with a high starting torque are indicated. The hysteresis comparator is utilized to compensate the phase delay of the back EMFs due to a Low-Pass Filter (LPF) and used to preventing multiple transition output from ripple or noise in terminal voltage. The rotor position is aligned at standstill for high starting torque without any additional sensor and information about motor parameters. Also, the stator current can be easily controlled by switching sequence of controller during alignment. The controller performance of APVM and corresponding simulation results are applied to sensor less control of BLDC motor and verified performance results using MATLAB/Simulink environment.

Keywords: NFSBBC, Photovoltaic (PV) System, MPPT/ P&O, BLDC motor, Hysteresis control, SPWM, APVM

1. INTRODUCTION

Renewable power is having more attention in power generation in increasing global warming today. In this especially solar power generation is a great attention in last decades [1]. In Existing system of solar power generation is arranged by series [2] and parallel [3] connection of solar cells, single and multiple inverters for high power and high efficiency conversion respectively. The main drawback of micro-inverter system is having low PV (Photovoltaic) power, large difference of voltage between input side and output side. This is because of shading effect or incompatible module of Photovoltaic Array so this is causes less efficiency and required high rating of power switches. The efficiency and maximum power point tracking of Photovoltaic Source is achieved by special converters such as Cuk and SEPIC converter are implemented to extract the power at maximum with high efficiency [4]. The notable drawback of above converter system is required many passive components in nature.

The less number of passive components with high efficiency range is obtained by applying four-switch buck-boost converter for medium power rating of solar power generation. Special features includes in four-switch inverter circuit are such as low rating of passive components rating, high step up and high step down capability compared with other power converters[5].

* Research Scholar, Department of Electrical and Electronics Engineering, St. Peter's University, Avadi, Chennai–600054, India, *Email: sundaramphd14@gmail.com*

** Department of Electronics and Communication Engineering, St. Peter's University, Avadi, Chennai–600054, India.

Even it has particular range of power conversion not in wide range. To overcome the above demerits a new enhancement of non-inverting polarity of Non-inverting four-switch buck-boost converter (NFSBBC) is proposed in this configuration because this is having less number of passive components with meet out the demands for power extraction, efficiency and wide power range of power extraction by suitable selection of passive device rating. Due to low power and high speed operation of drive, Brushless DC Motor (BLDC) motor is applied for much more application in recent decades such as automotive, computer, industrial, household and recently in heavy drives also and etc [6]. Classical approach of sensor control using Hall Effect for Brushless DC Motor (BLDC) is applied to sensing position of rotor [7]. So this is used to drive exact commutation of current. The influence of maintenance and cost is the reason for developing a sensor less algorithm to special drives especially in Brushless DC motor Drives (BLDC). The sensor less control loop is provides a less maintenance cost and high reliability in nature.

This paper is proposed a sensor less control of brushless DC motor using hysteresis comparator by overcoming the limitation of sensor control loop. Control loop drives accurate commutations of current by appropriate switching pulse generation and increasing inner loop speed matching to outer loop of system. A new enhanced approach of maximum power extraction for photovoltaic system was implemented using non-inversion four-switch buck boost converter. The proposed MPPT approach is reached maximum efficiency, reliability and high ratio of power conversion with less number of passive device and rating. The effectual performance of MPPT using proposed converter topology and sensor-less approach using hysteresis band control and details is given in chapter III and chapter IV respectively.

2. AUTONOMOUS PHOTOVOLTAIC SYSTEM USING MPPT TOPOLOGY

The presented a new enhanced Non-inverting four switch buck boost converter (NFSBBC) using perturbs and observer based MPPT topology is proposed in proposed autonomous photovoltaic systems. The present autonomous system is applied for Brushless DC Motor control. Four switch converter design and details and Autonomous photovoltaic module is described below.

2.1. Non-inverting four switch buck-boost converter (NFSBBC)

The Non-inverting Four Switch Buck Boost Converter (NFSBBC) is a family of buck boost converter topology. But this is separated from classical buck-boost, SEPIC and Cuk converter in the form of reliability, efficiency, high step-up and step-down capability, less number of passive components and low range of components. The design aspects of proposed converter system are obtained by voltage-second balanced theorem. The gain of voltage G_V is obtained by

$$G_V = \frac{V_{out}}{V_{PV}} = \frac{D_1}{1 - D_2} \tag{1}$$

D_1, D_2 are derived duty cycles for S_A and S_B switch which presented in proposed converter system. S_{A1}, S_{A2} are rectifier switches for S_A, S_B switches. Pulse width modulation is designed on the basis of continuous and discontinuous operation. The nature of proposed converter topology is discontinuous power flow in between buck (step-down) and boost (step-up) operation. So this discontinuous is needed to change continuous operation for smooth and steady state operation of voltage. Carrier overlapping scheme is introduced for reference signal comparison to delivered exact pulse duty cycles of D_1, D_2 [8]. Reference signal generation and magnitude is important phenomena for proposed Buck-Boost operation and also high step-up ratio. So this is derived by adequate MPPT algorithm using perturb and observer method [9]. Due to the condition of photovoltaic system proposed MPPT extract power by using adequate reference signal generation for NFSBBC circuit and duty cycles D_1, D_2 are shown in Fig. 1 and Fig. 2.

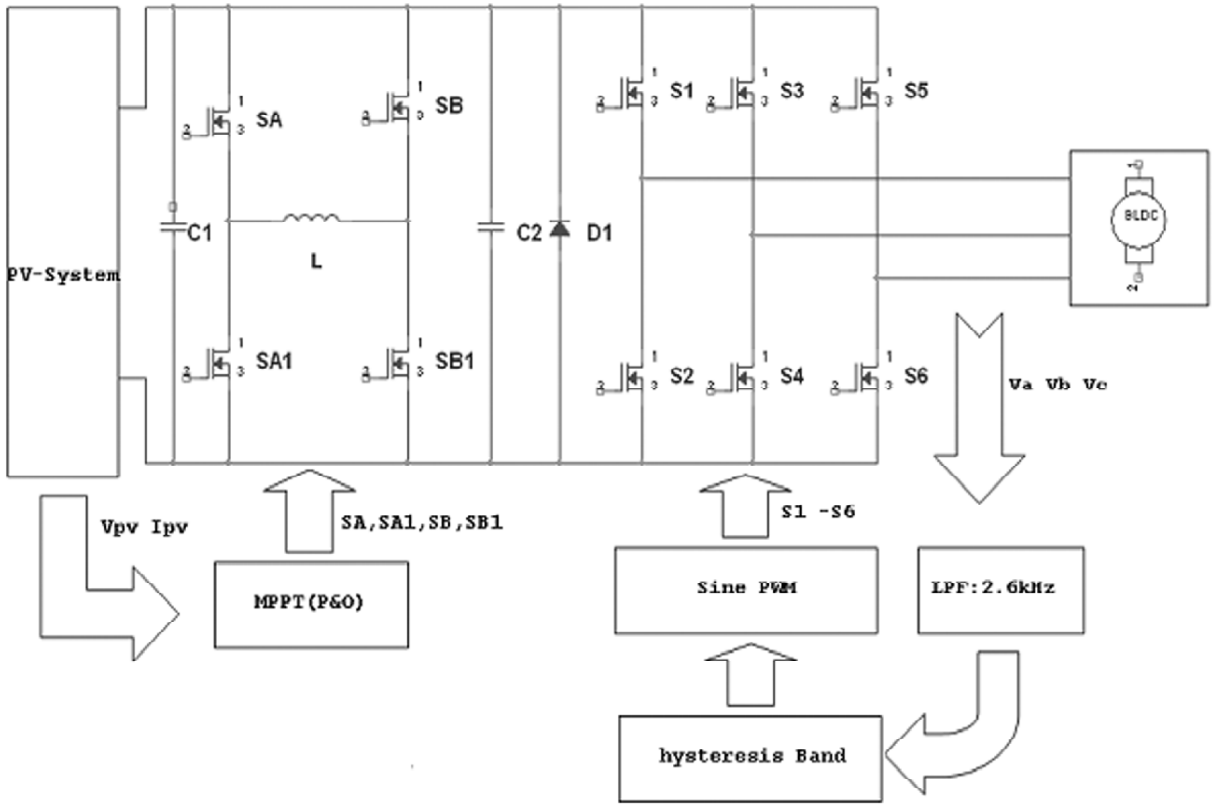

Figure 1: A new Enhanced Photovoltaic Power Generation for BLDC Motor using sensor-less Hysteresis PWM Control

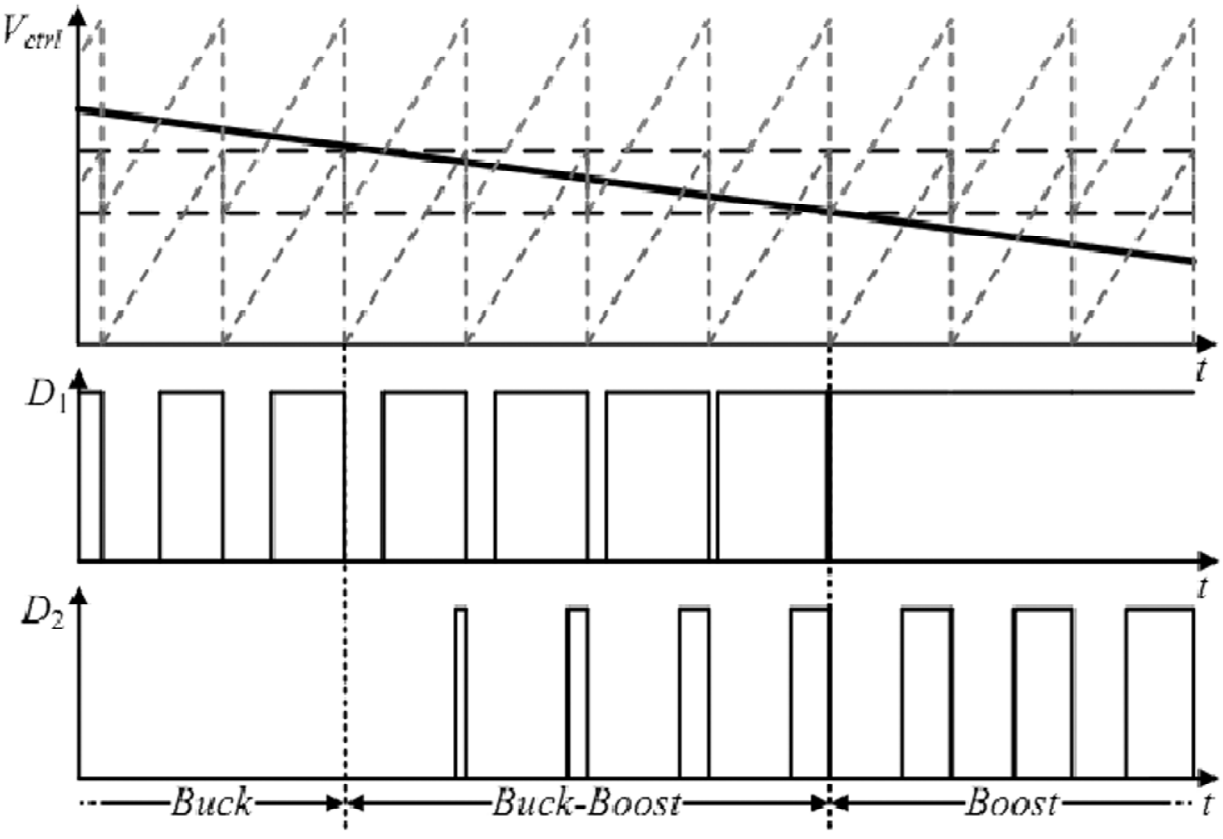

Figure 2: Control Pulses for Non-inverting Four Switch Buck Boost converter (NFSBBC)

2.2. Autonomous photovoltaic system using NFSBBC circuit

The voltage gain is derived by using transfer function from load side voltage to source side voltage transfer function G_{oi} and Obtained duty cycle to input voltage transfer function using continuous conduction mode is represented by G_{i1}, G_{i2}. The equivalent circuit of Non-inverting circuit is an ideal form shown in Fig. 3. Load side voltage of circuit and source side voltage of circuit is represented by fixed voltage source converter.

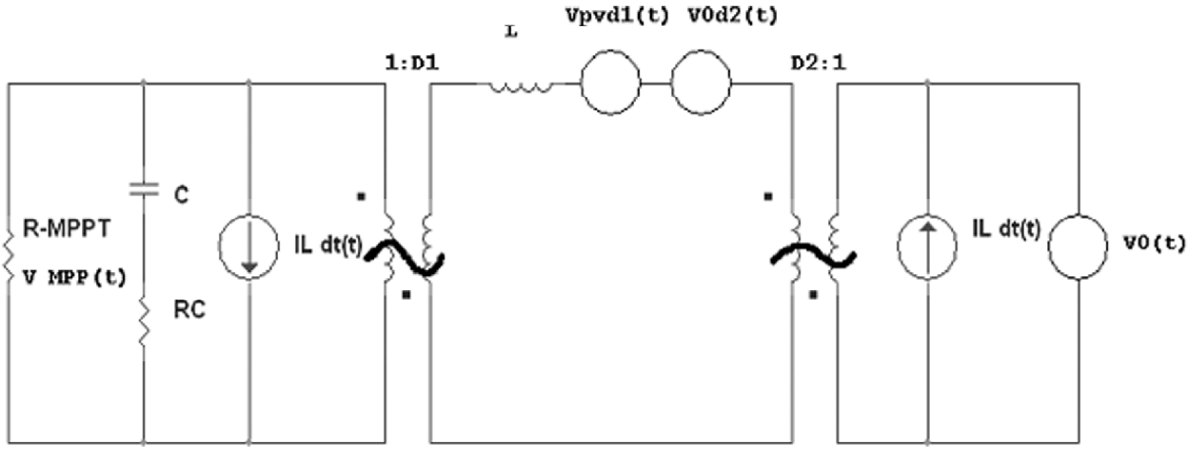

Figure 3: Equivalent Circuit for Autonomous Photovoltaic System

In equivalent circuit, is denoted as input series resistance for capacitor across input side of transfer function. Maximum value of voltage is derived using perturb and observer method by

$$\left.\frac{\partial i_{PV}}{\partial V_{PV}}\right|_{MPP(PV)} = \frac{1}{R_{MPP(PV)}} \tag{2}$$

The detailed deviation of mathematical function is expressed by following

$$G_{oi}(s) = \left.\frac{\hat{V}_{PV}}{\hat{V}_o}\right|_{\substack{\hat{d}_{1=0} \\ \hat{d}_{2=0}}} = \frac{1-D_2}{D_1}\frac{\left(1+\dfrac{s}{w_{z1}}\right)}{\left(1+\dfrac{s}{qw0}\left(\dfrac{s}{w_0}\right)^2\right)} \tag{3}$$

$$G_{i1}(s) = \left.\frac{\hat{V}_{PV}}{\hat{d}_1}\right|_{\substack{\hat{V}_{0=0} \\ \hat{d}_{2=0}}} = \frac{-V_{PV}}{D_1}\frac{\left(1+\dfrac{s}{w_{z1}}\right)\left(1+\dfrac{s}{w_{z2}}\right)}{\left(1+\dfrac{s}{qw0}\left(\dfrac{s}{w_0}\right)^2\right)} \tag{4}$$

$$G_{i2}(s) = \left.\frac{\hat{V}_{PV}}{\hat{d}_2}\right|_{\substack{\hat{V}_{0=0} \\ \hat{d}_{1=0}}} = \frac{-V_0}{D_1}\frac{\left(1+\dfrac{s}{w_{z1}}\right)}{\left(1+\dfrac{s}{qw0}\left(\dfrac{s}{w_0}\right)^2\right)} \tag{5}$$

Where

$$w_0 = \sqrt{\frac{R_{MPP(PV)D_1^2}}{LC\left(R_{MPP(PV)} + R_C\right)}} \tag{6}$$

$$Q = \frac{1}{\left(\frac{L}{R_{MPP(PV)D^2}} + R_c C\right)\sqrt{\frac{R_{MPP(PV)D_1^2}}{LC\left(R_{MMP(PV)} + R_c\right)}}} \tag{7}$$

$$W_{z1} = \frac{1}{R_c C} \tag{8}$$

$$W_{z2} = \frac{V_{PV} D_1}{L I_L} \tag{9}$$

3. PROPOSED SENSOR-LESS CONTROL USING HYSTERESIS COMPARATOR

The proposed controller design circuit, algorithm of sensor-less control and three phase reference signal generation for hysteresis-PWM generation are described in below and control loop structures are design is shown in Fig. 4.

The substantial basics of present sensor less control algorithm in drives control system is about finding out machine's rotor position by sensing of phase voltage, phase current and back EMF sensing. This proposed system loop contained similar loop design except emf sensing structure over natural classical scheme. The

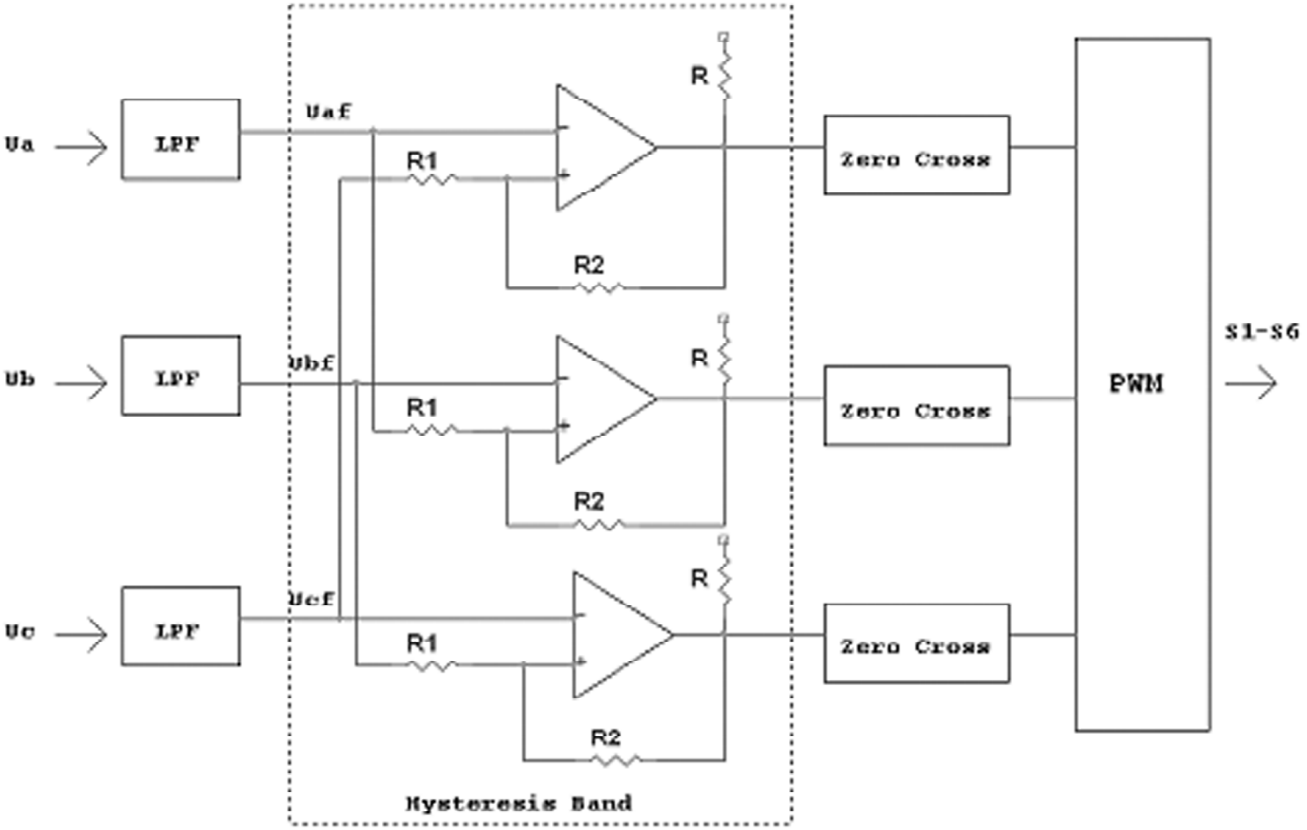

Figure 4: Structure of Hysteresis PWM control Loop

enhancement of sensor less control structure shown in Fig. 4 is initially three phase voltages are measured and given to Low Pass Filter (LPF). Low pass filter is used as noise suppression or neglect.

Voltage reference signal is denoted by (U_{reff}) is obtained by low pass filter and this is compared with U_{reff}*. The comparison between actual controller voltage source and reference signals is closed to nature. Reference of voltage is naturally close to back emf so we can easily identify about commutation of Brushless DC Motor (BLDC) to provide exact excitation for two phases of Brushless DC Motor (60° – 120°) at a time. The signal comparison is given to as Hysteresis band pass filter input. Presented hysteresis based band pass filter circuit provides an adequate reference signals for pulse width modulation generation using sine PWM topology. This type of pulse width modulation is separated from classical logic operator based pulse generation method. Important features of hysteresis band to provide exact gate pulse signals to control of commutation current which present on phase line and inverter circuit. The working principles of hysteresis band comparator with respect to time which is shown in Fig. 5.

The present low pass filter cut-off frequency is can easily affect torque signal and speed signal on Brushless DC Motor load performance [10]. Harmonics and noises are easily appear by variation of cut-off frequency so utilizing of low pass filter in control circuit is in desired frequency limits in the range 2.6 kHz.

The phase difference between filtered output signals and actual signals draws from phase line of inverter applied across hysteresis band to obtained desired commutation of reference signals. Phase A is applied to inverter leg to lead signal in desired range and other hand phase C is applied through Resistance of phase signal. The phase difference between filter and resistance is expressed by

$$U_{da} = -V_{af} + \frac{1}{n+1}U_{0a} + \frac{n}{n+1}V_{cf} \tag{10}$$

Where, V_{af}, is a filtered reference signal, $n = \frac{R_1}{R_L}$ is a differenced signal is obtained by resistance of phase line in C or A. Equation in above (10) U_{0a} is positive means U_{0a} = + U_{sat}. If the condition is negative

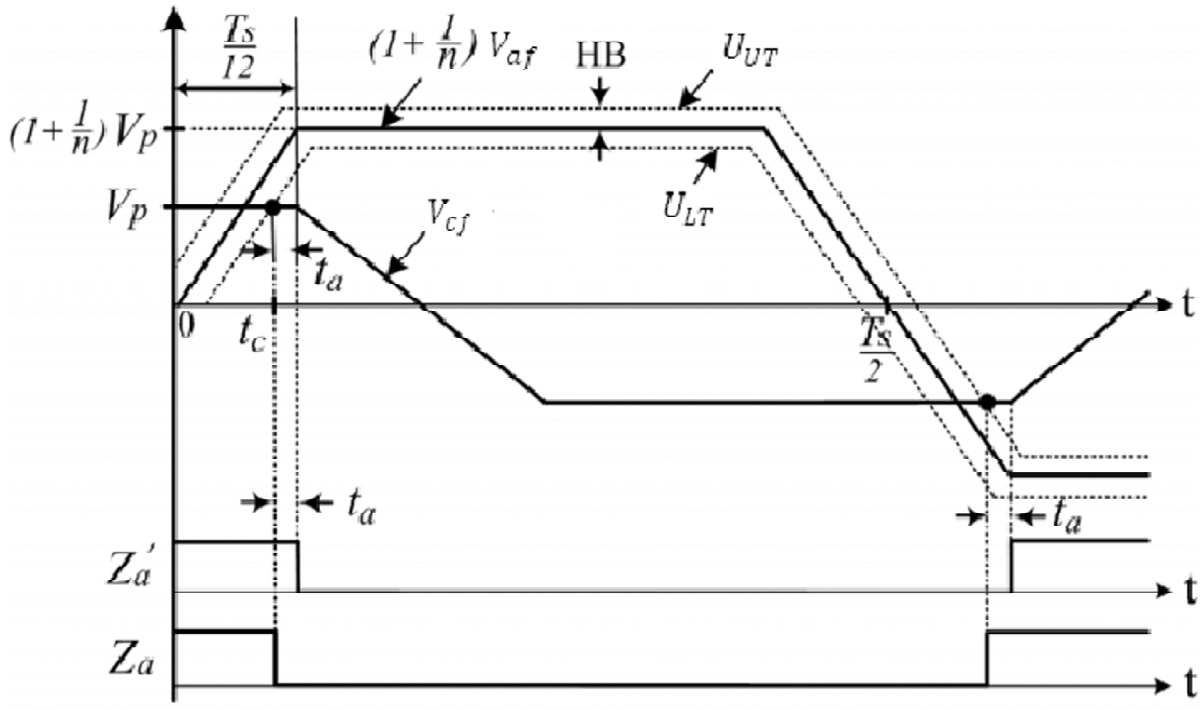

Figure 5: principles of proposed hysteresis pulse width modulation

for phase terminals of C is denoted by V_{cf}. At $U_{0a} = -U_{sat}$, load terminal voltage U_{0a} switches back to $+U_{sat}$, when differential form of voltage is positive (10) i.e the condition derived by following manner,

$$V_{cf} > \left(\left(1+\frac{1}{n} \right) V_{af} + \left(\frac{1}{n} \right) U_{sat} \right) \tag{11}$$

$\left(\frac{1}{n} \right) U_{sat}$ In equation (10) and (11) is a hysteresis band which is determined by output voltage level U_{sat} and resistance ration which is denoted by n. in equation (10) and (11) right side of equation is multiplied by upper and lower level of threshold voltage of U_{UT} and U_{LT} respectively. Those are multiplied by $\left(1+\frac{1}{n} \right)$ [10] is denoted by,

$$U_{UT} = \left(\left(1+\frac{1}{n} \right) V_{af} + \left(\frac{1}{n} \right) U_{sat} \right) \text{(For upper threshold value)} \tag{12}$$

$$U_{LT} = \left(\left(1+\frac{1}{n} \right) V_{af} + \left(\frac{1}{n} \right) U_{sat} \right) \text{ (For lower threshold value)} \tag{13}$$

The load terminal voltage of $+U_{sat}$ and V_{cf} is smaller than U_{LT} then switches to $-U_{sat}$. The same condition is bellow of U_{LT} then terminal voltage is $+U_{sat}$. The real commutation signal for phase A is *Za* is generated from low pass filter at t_a. Time function of U_{LT} is described by

$$U_{LT}(t) = \frac{12\ V_{\max}}{T_s} \left(1+\frac{1}{n} \right) t - \left(\frac{1}{n} \right) V_{sat} \tag{14}$$

Where V_{max}, is a maximum voltage of terminals, T_s is total time of performance of terminal voltage. Using equation (14), time interval of t_c at the terminals between U_{LT} and V_{cf} is expressed by

$$t_c = \frac{T_s}{2} \left(\frac{n}{1+n} + \frac{1}{1+n} \times \frac{U_{sat}}{V_{max}} \right) \tag{15}$$

t_a, is a interval between t_c and $\frac{T_s}{2}$ is expressed by

$$t_a = \frac{T_s}{2} - t_c \tag{16}$$

In equation (16), equation (15) is applied and described about angle of phase A is θ_a by

Table I

U_0	$U_0 - 120°$	$U_0 - 240°$	$U_1 - 120°$	$U_1 - 240°$

$$\theta_a = w_{ta} = \frac{T_s}{2} \left(\frac{1}{1+n} \right) \frac{1-U_{sat}}{V_{max}} \tag{17}$$

Angle θ_a is inversely proportional to resistance value on phase line. If resistance decreases then angle will be increase and maximum of voltage V_{max} also decreases. Lagging of signal is can be compensated by

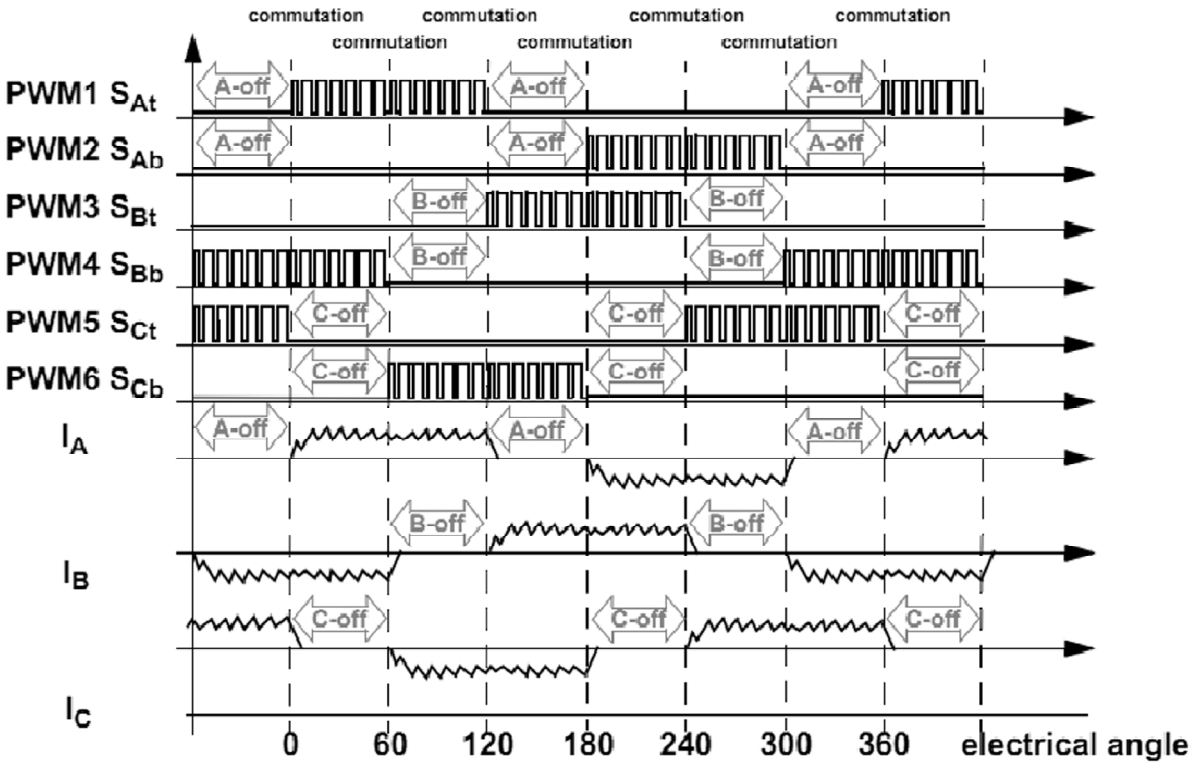

Figure 6: Proposed brushless DC Motor commutation using Sine PWM

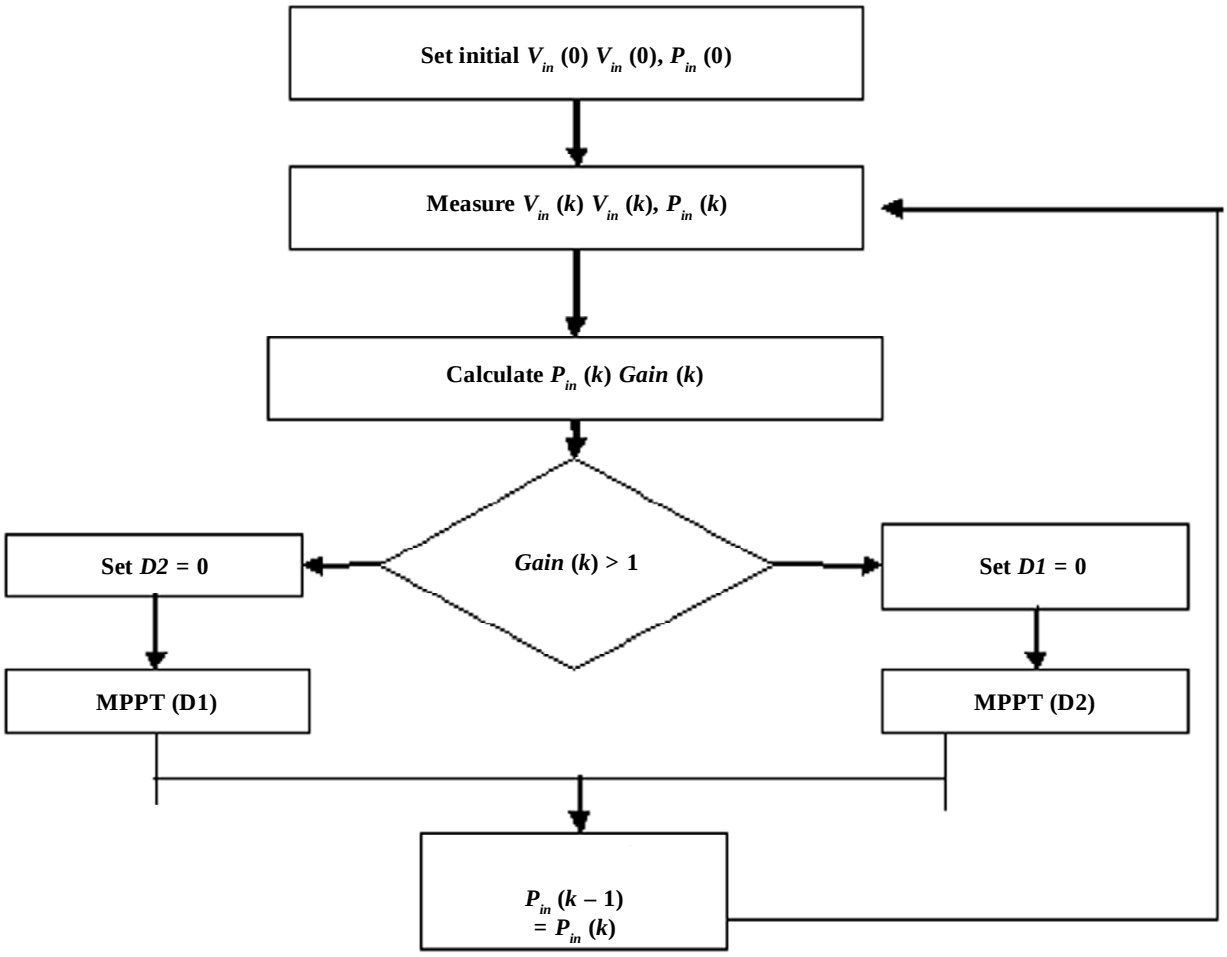

Figure 7: Flow chart for MPPT using perturb and observer method

Table 2
Specification of parameters

Converter specification	
Name	*Value*
$V_{PV}(V)$	25
$I_{PV}(A)$	2.5
$P_{PV}(W)$	62
$V_{out}(V)$	60
$L(\mu H)$	800
$C1(\mu F)$	200
$C2(\mu F)$	200
$R(m\Omega)$	50
$L(mH)$ grid side	1
$C1(nF)$ grid side	1
Motor Specification	
Rated voltage(V)	60
Rated Current(A)	3A
Nominal speed (rpm)	3000
Stator Resistance(Ω)	0.19
Stator Inductance(mH)	0.835
Rotor moment of inertia J(kg.m^2)	1.9959μ

varying resistance value n across phase terminals. Low pass filter is range limits are fixed in +1V, resistance value is varied up to 1.2; maximum peak voltage V_{max} is 1.2 V. The table I: is shown about a single sequence for proposed three phase inverter and Sequence UVW are applied to three phase inverter for forward direction. WUV sequence is taken in account for reverse direction. Given sequence table is applied and used in generated pulse width modulation which is shown in Fig. 6.

4. SIMULATION RESULTS

The present converter system is provides a maximum power generation from solar power using perturb and observer method shown in Fig. 7 and this is applied to brushless DC motor control using sensor less based hysteresis PWM generation. The circuit of proposed implementation is developed using MATLAB/Simulink which is shown in Fig. 8. Present converter of buck boost conversion capability of voltage performance across DC-Link voltage is shown in Fig. 9. Proposed hysteresis band used to control of lag and lead of phase voltage angle to control of speed and torque of brushless DC Motor is specification is in Table-II. This controller is cost effective compared with sensor and other sensor less method because this is required phase voltage alone to finding rotor‘s condition and adequate pulse width modulation generation. The control performance is verified using simulation result through motor performance is shown in Fig. 10, 11 and 12.

5. CONCLUSION

The topology of Non Inverting Four Switch Buck Boost Converter (NFSBBC) is provided a maximum of power extraction from solar panel. The special features of proposed NFSBBC are having less number of components with high efficiency and this is used to provide continuous power supply to three phase inverter fed brushless DC Motor. Buck boost operation of present converter is operated is based on condition of solar panel and internal generation capacity. Extraction of power is improved by proposed perturb and

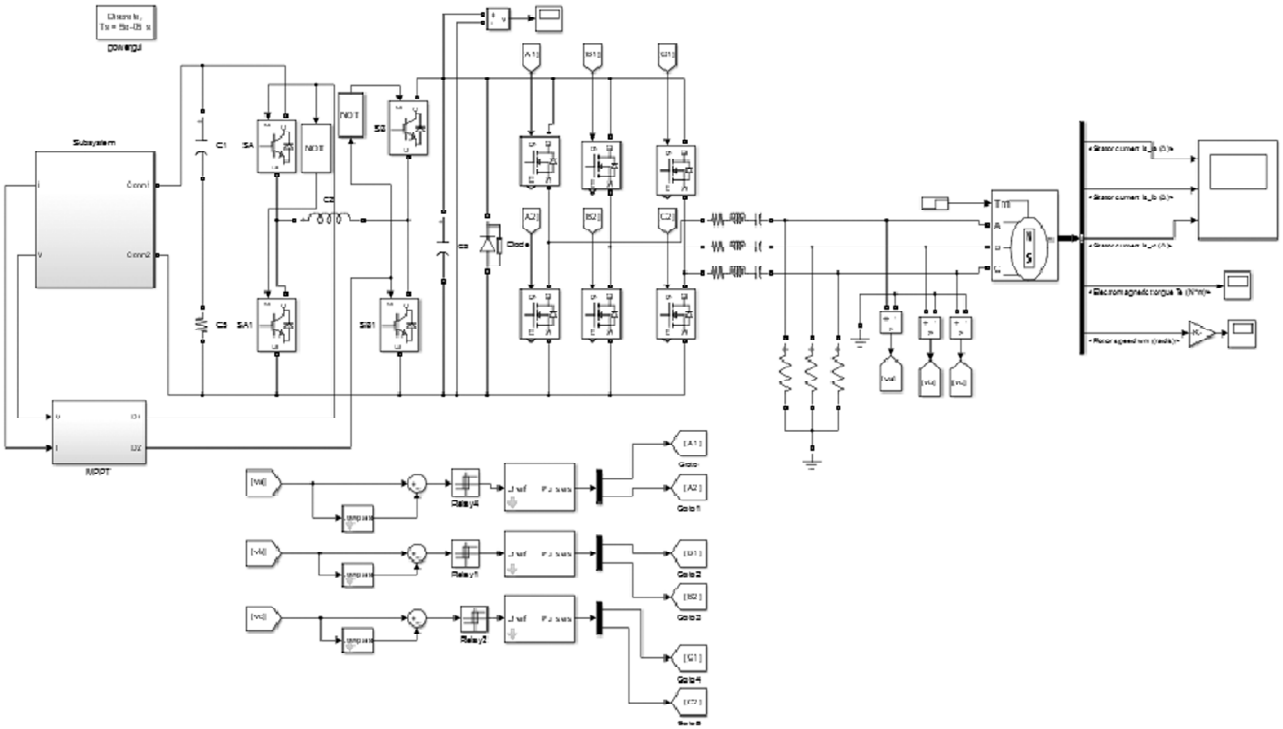

Figure 8: Simulation implementation circuit for proposed topology

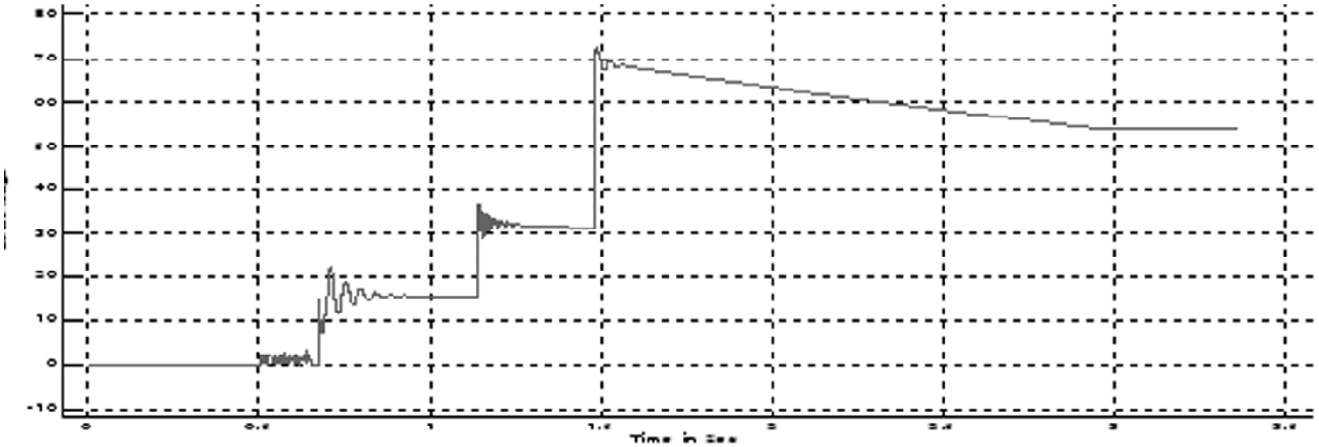

Figure 9: DC-Link Voltage of non inverting four switch buck boost converter (a)

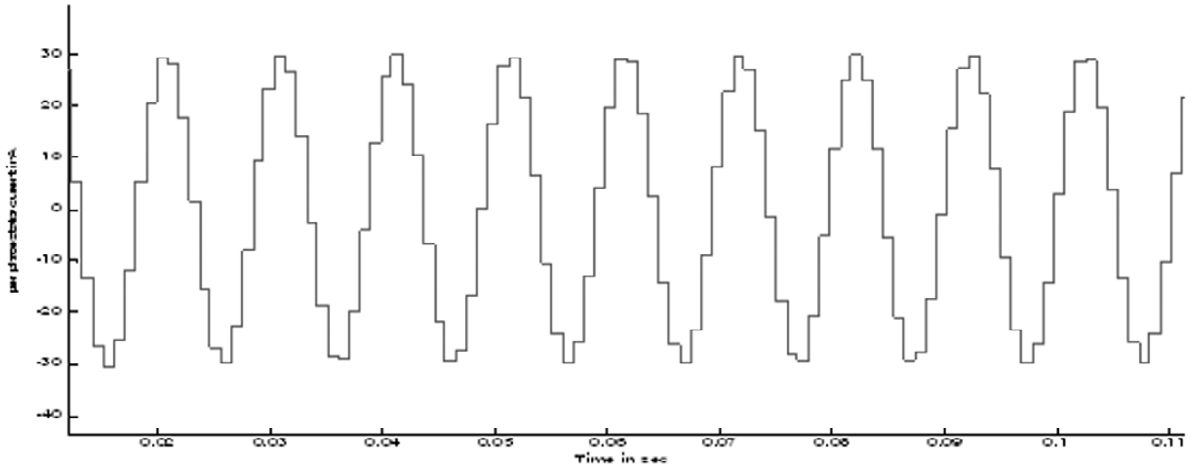

(a)

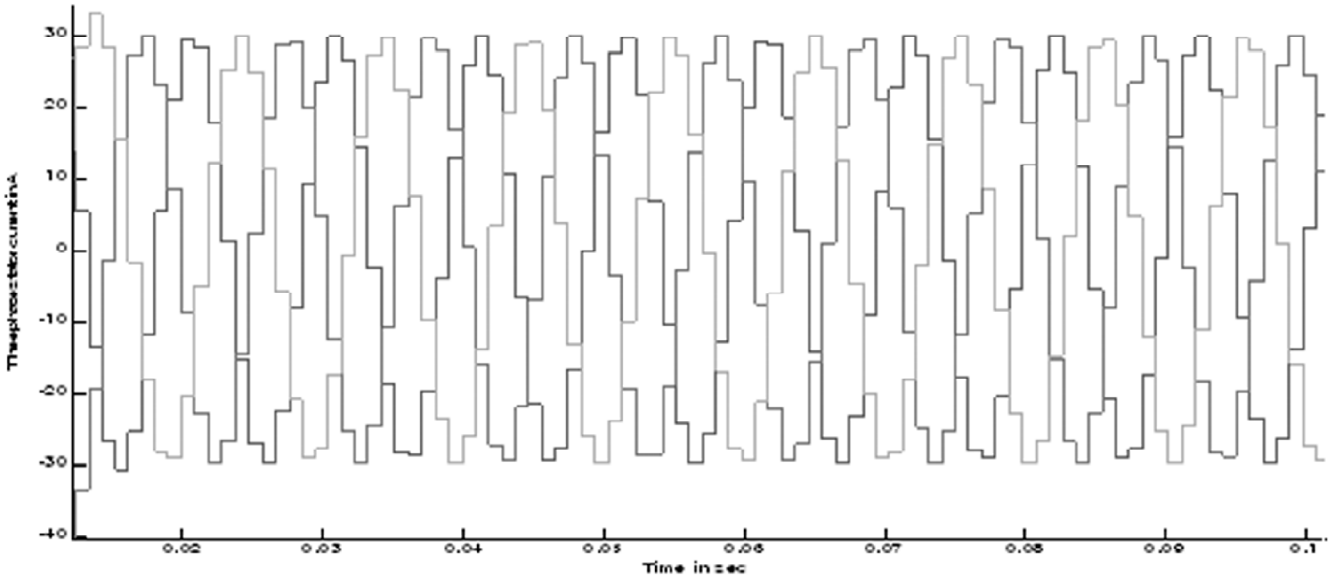

(b)

Figure 10: stator phase current: (a) per phase stator current signals (b) combined three phase signal

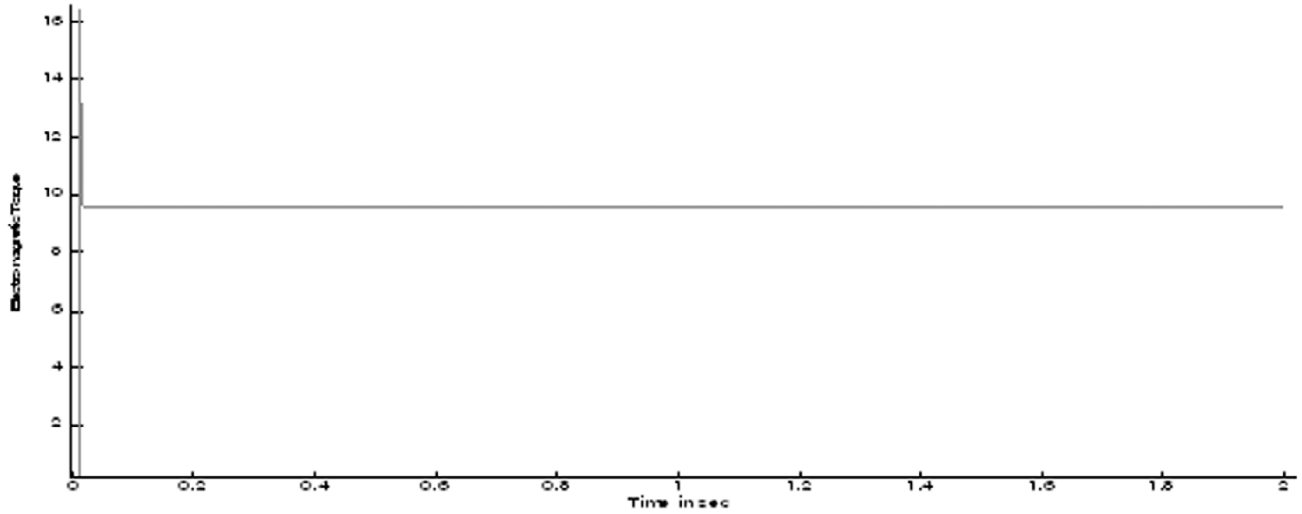

Figure 11: Electromagnetic torque performance

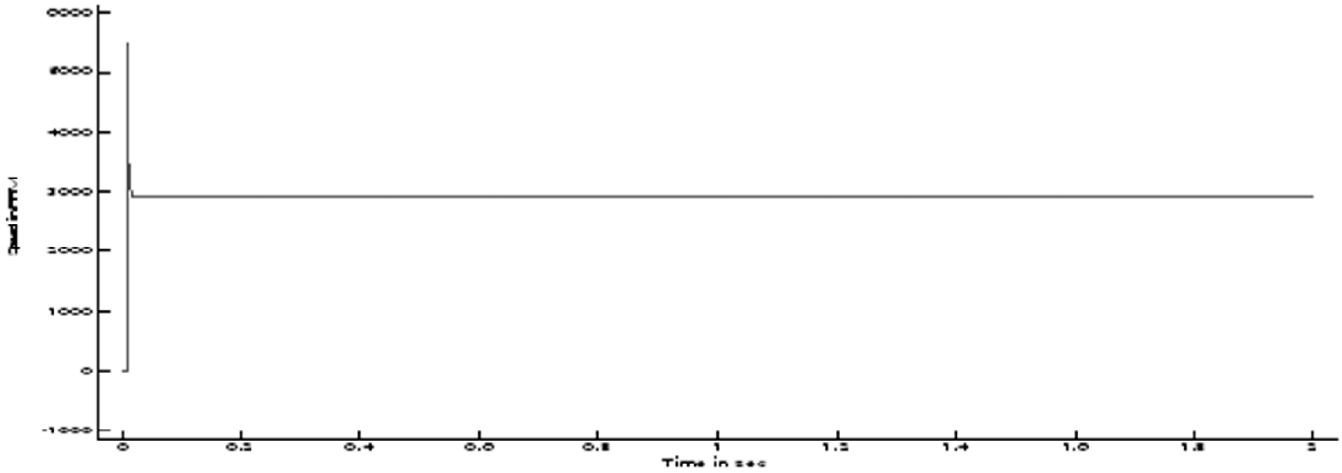

Figure 12: Speed performance of brushless DC Motor in RPM

observer method and also brushless DC Motor is controlled by effective sensor less based hysteresis PWM control. The present hysteresis band is used to control of phase voltage angle so we can obtained better electromagnetic torque and speed of brushless DC Motor performance. Buck-boost operation and performance of present converter and enhanced hysteresis based sensor less PWM control topology performance also given in details in this paper. Topology was implemented using MATLAB/Simulink and result was proved in the improvement in the form of converter and motor performance over existing topology.

REFERENCES

[1] Chen, Cheng-Wei, Kun-Hung Chen, and Yaow-Ming Chen. "Modeling and controller design of an autonomous PV module for DMPPT PV systems." Power Electronics, IEEE Transactions on 29.9 (2014): 4723-4732.

[2] Walker, Geoffrey R., and Paul C. Sernia. "Cascaded DC-DC converter connection of photovoltaic modules." Power Electronics, IEEE Transactions on 19.4 (2004): 1130-1139.

[3] Gules, Roger, et al. "A maximum power point tracking system with parallel connection for PV stand-alone applications." Industrial Electronics, IEEE Transactions on 55.7 (2008): 2674-2683.

[4] Mangu, B., and B. G. Fernandes. "Efficiency improvement of solar-wind based dual-input Cuk-SEPIC converter for telecom power supply." IECON 2012-38th Annual Conference on IEEE Industrial Electronics Society. IEEE, 2012.

[5] Orellana, Marcos, Stephane Petibon, Bruno Estibals, and Corinne Alonso. "Four Switch Buck-Boost Converter for Photovoltaic DC-DC power applications." In IECON 2010-36th Annual Conference on IEEE Industrial Electronics Society, pp. 469-474. IEEE, 2010.

[6] Kim, Tae-Hyung, and Mehrdad Ehsani. "Sensorless control of the BLDC motors from near-zero to high speeds." Power Electronics, IEEE Transactions on 19.6 (2004): 1635-1645.

[7] Wu, Yuanyuan, et al. "Position sensorless control based on coordinate transformation for brushless DC motor drives." Power Electronics, IEEE Transactions on 25.9 (2010): 2365-2371.

[8] Y.J. Lee, A. Khaligh, and A. Emadi, "A Compensation Technique for Smooth Transitions in a Noninverting Buck–Boost Converter," IEEE Transactions on Power Electronics, vol. 24, no. 4, pp. 1002-1015, April 2009.

[9] N. Femia, G. Petrone, G. pagnuolo, and Vitelli, "Optimization of perturb and observe maximum power point tracking method," IEEE Transactions on Power Electronics, vol. 20, no. 4, pp. 963-973, July 2005.

[10] Chun, Tae-Won, et al. "Sensorless control of BLDC motor drive for an automotive fuel pump using a hysteresis comparator." Power Electronics, IEEE Transactions on 29.3 (2014): 1382-1391.